Study of the process $e^+e^- \to K^+K^-\pi^0$ in the center-of-mass energy range 1.2–2 GeV with the CMD-3 detector

A. L. Erofeev[1,2,*], R. R. Akhmetshin[1,2], A. N. Amirkhanov[1,2], A. V. Anisenkov[1,2], V. M. Aulchenko[1,2], V. Sh. Banzarov[1], N. S. Bashtovoy[1], D. E. Berkaev[1,2], A. E. Bondar[1,2], A. V. Bragin[1], S. I. Eidelman[1,2,5], D. A. Epifanov[1,2], L. B. Epshteyn[1,2,3], G. V. Fedotovich[1,2], S. E. Gayazov[1,2], A. A. Grebenuk[1,2], S. S. Gribanov[1,2], D. N. Grigoriev[1,2,3], F. V. Ignatov[1,2], V. L. Ivanov[1,2], S. V. Karpov[1], A. S. Kasaev[1], V. F. Kazanin[1,2], I. A. Koop[1,2], A. A. Korobov[1,2], A. N. Kozyrev[1,3], E. A. Kozyrev[1,2], P. P. Krokovny[1,2], A. E. Kuzmenko[1,2], A. S. Kuzmin[1,2], I. B. Logashenko[1,2], A. P. Lysenko[1], P. A. Lukin[1,2], K. Yu. Mikhailov[1], V. S. Okhapkin[1], A. V. Otboev[1], E. A. Perevedentsev[1,2], Yu. N. Pestov[1], A. S. Popov[1,2], G. P. Razuvaev[1,2], A. A. Ruban[1], N. M. Ryskulov[1], A. E. Ryzhenenkov[1,2], A. V. Semenov[1,2], A. I. Senchenko[1], Yu. M. Shatunov[1], V. E. Shebalin[1,2], D. N. Shemyakin[1,2], B. A. Shwartz[1,2], D. B. Shwartz[1,2], A. L. Sibidanov[1,4], E. P. Solodov[1,2], V. M. Titov[1], A. A. Talyshev[1,2], A. I. Vorobiov[1], and Yu. V. Yudin[1,2]

[1]Budker Institute of Nuclear Physics, SB RAS, Novosibirsk, 630090, Russia
[2]Novosibirsk State University, Novosibirsk, 630090, Russia
[3]Novosibirsk State Technical University, Novosibirsk, 630092, Russia
[4]University of Victoria, Victoria, BC, Canada V8W 3P6
[5]Lebedev Physical Institute RAS, Moscow, 119333, Russia

Abstract. The process $e^+e^- \to K^+K^-\pi^0$ has been studied in the center-of-mass energy range from 1.2 to 2 GeV using a 80.6 pb^{-1} data sample collected with the CMD-3 detector at the electron-positron collider VEPP-2000. Preliminary results of the cross-section measurement are presented.

1 Introduction

The process $e^+e^- \to K^+K^-\pi^0$ has been studied up to now with low statistical accuracy by the DM2 [1] and BABAR [2] experiments. The data on the total cross section of this process are needed for precise calculation of the hadronic contribution to the muon $g-2$ and $\alpha(M_Z^2)$. A detailed study of the production dynamics will improve our understanding of strong interactions at low energies and theoretical models of light hadron production.

The general-purpose detector CMD-3 is described in detail elsewhere [3]. Its tracking system consists of the cylindrical drift chamber (DC) and double-layer multiwire proportional Z-chamber with both subsystems installed inside a thin superconducting solenoid with 1.3 T magnetic field. Both subsystems are used to generate a trigger signal. The DC contains 1218 hexagonal cells and performs a measurement of the momentum, polar (θ) and azimuthal (ϕ) angles of the charged particles. The barrel electromagnetic calorimeters placed outside the solenoid are based on liquid xenon (LXe) and CsI crystals with a thickness of 5.4 X_0 and

*e-mail: andrikola@yandex.ru

8.1 X_0, respectively. The endcap calorimeter is based on BGO scintillation crystals with a thickness of 13.4 X_0.

2 Data analysis

Signal events contain two charged kaons and two photons produced in the π^0 decay. Thus candidates with two tracks with zero total charge and at least two photons with energies more than 20 MeV are selected. We require the tracks to originate from the beam interaction region in a 10 cm neighborhood along the beam axis with an impact parameter not larger than 0.4 cm. These limitations are reinforced by a selection condition for noncollinear tracks expressed by the inequalities $||\phi_1 - \phi_2| - \pi| > 0.15$ rad and $|\theta_1 + \theta_2 - \pi| > 0.25$ rad, allowing efficient rejection of cosmic rays and beam background events. The tracks are also required to pass the central part of the DC for the best agreement between experiment and simulation: $|\theta - \pi/2| < 0.8$ rad.

Now we turn to higher-level selection, the main purpose of which is to separate the signal process events from the events of other possible channels of e^+e^- annihilation. To avoid cumbersome mathematical expressions, let us denote the energy of a particle with mass m and three-momentum $\mathbf{p}$ by a symbol $\mathcal{E}(\mathbf{p}, m)$. Then the track momenta $\mathbf{p}_1$ and $\mathbf{p}_2$ must satisfy an inequality $\mathcal{E}(|\mathbf{p}_1| - |\mathbf{p}_2|, m_{\pi^0}) \leq \sqrt{s} - \mathcal{E}(\mathbf{p}_1, m_K) - \mathcal{E}(\mathbf{p}_2, m_K) \leq \mathcal{E}(|\mathbf{p}_1| + |\mathbf{p}_2|, m_{\pi^0})$ resulting from the kinematics of the process. We impose this restriction on the measured track momenta. Event selection is also performed on the total momentum $P = |\mathbf{p}_1 + \mathbf{p}_2 + \mathbf{k}_1 + \mathbf{k}_2|$ and the total energy difference $\Delta E = |\sqrt{s} - \mathcal{E}(\mathbf{p}_1, m_K) - \mathcal{E}(\mathbf{p}_2, m_K) - |\mathbf{k}_1| - |\mathbf{k}_2||$, where $\mathbf{p}$ and $\mathbf{k}$ denote the three-momenta of the track and the photon, respectively. We require $P < 0.16$ GeV/c and $\Delta E < 0.18$ GeV.

We perform a 4C-kinematic fit (KF) for every combination of a photon pair and two charged tracks in an event requiring the energy-momentum conservation without applying a π^0 mass constraint. The fit reconstructs the momenta and angles of the selected tracks and photons. The photon pair producing the lowest χ^2 is retained if the reconstructed energies of both quanta $E_\gamma > 40$ MeV.

An essential part of background comes from the processes with charged pions, especialy from a process $e^+e^- \to \pi^+\pi^-\pi^0\pi^0$. The tracks of pions and kaons are well separated by ionization losses in the DC unless the momenta of these particles are higher than 500 MeV/c. To suppress these parasitic processes at high $\sqrt{s}$ we have to use kinematics additionally.

A significant background contribution, as simulation shows, is also represented by the processes of e^+e^- annihilation into final states: $K^+K^-\pi^0\pi^0$, $K^0_S K\pi$, $K^0_L K\pi$ and $K^+K^-\gamma$. The events of the former are well separated at high energies by the squared recoil mass of the tracks $M^2_{rec} = (\sqrt{s} - |\mathbf{p}_1| - |\mathbf{p}_2|)^2 - (\mathbf{p}_1 + \mathbf{p}_2)^2$, where $\mathbf{p}_1$ and $\mathbf{p}_2$ are track momenta before kinematic reconstruction.

For further background suppression use was made of the Boosted Decision Tree (BDT) method. In accordance with stated above we accepted as BDT arguments the ionization losses dE/dx of the tracks in the DC, the track momenta after kinematic reconstruction, the momenta and angles θ of the photons after KF and the parameter M^2_{rec}. To train and test the classifier we use GEANT4-based [4] Monte Carlo simulation of the signal and all mentioned background processes. Shown in Figure 1 are distributions of the BDT response for experimental and simulated data with the latter normalized to luminosity. Due to the overlapping of the dE/dx distributions of different particles with the track momenta over 500 MeV/c, the background suppression quality drops significantly at high energies as also can be seen from the Figure 1. In order to improve this situation we limit the possible values of the KF χ^2 and M^2_{rec} as shown in Figure 2 by the dashed lines. The resulting distribution of the reconstructed photon pair invariant mass $M_{\gamma\gamma}$ vs the BDT response is shown in Figure 3

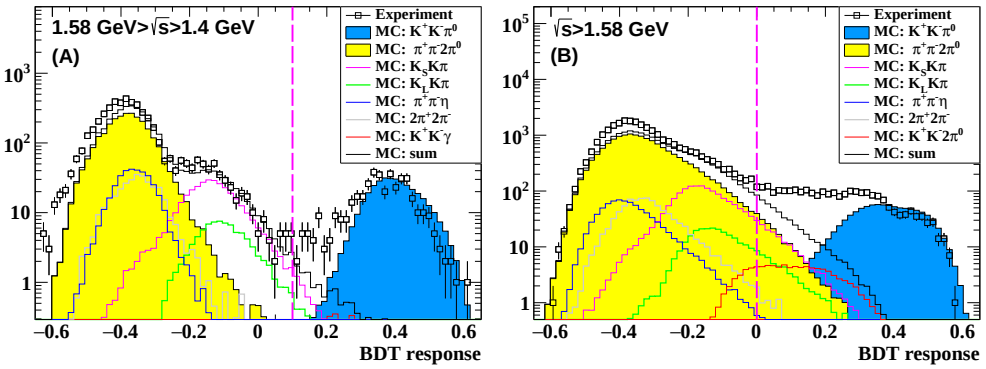

Figure 1. Separation of signal and background events in the range of medium energies (A) and at high energies (B). The dashed lines designate cut lines. The figure also shows the contributions of the main background processes expected from the simulation with normalization to luminosity. Separation of the signal and background events using the BDT response becomes inefficient at high energies.

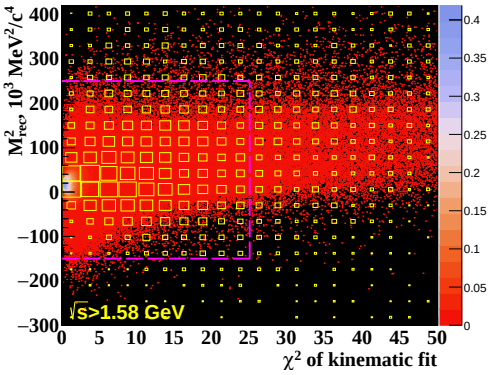

Figure 2. Squared recoil mass M^2_{rec} vs χ^2 of kinematic reconstruction for the simulation (scatter-plot) and the experimental data (box diagram). The dashed lines correspond to applied criterion.

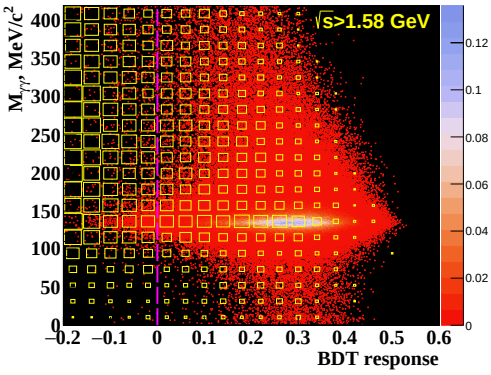

Figure 3. Reconstructed photon pair invariant mass $M_{\gamma\gamma}$ vs BDT response for the simulation (scatter-plot) and the experimental data (box diagram). The dashed line designates cut line.

where we can see the presence of the signal. However, after all the selections are applied, the number of background events is comparable to the yield of the studied process at high $\sqrt{s}$.

The signal yield at each energy point is determined from a fit of the photon pair invariant mass distribution for events that satisfy all mentioned above selection criteria. More specifically, we proceed as follows. The energy range is divided into several intervals. The invariant mass spectrum of selected experimental events from each energy interval is approximated by a function $F(x) = p_0 F_{2K\pi}(x) + p_1 F_{4\pi}(x) + p_2 + p_3 x + p_4 x^2 \equiv p_0 F_{2K\pi}(x) + F_{bg}(x)$, where p_i are parameters of approximation, $F_{2K\pi}$ and $F_{4\pi}$ denote functions describing the contributions of the signal and the process $e^+e^- \to \pi^+\pi^-\pi^0\pi^0$, which are determined from the simulation. The $M_{\gamma\gamma}$ spectrum at each energy point is fitted by a function $F(x) = q_0 F_{2K\pi}(x) + q_1 F_{bg}(x)$, where $F_{2K\pi}$ is taken from the simulation for given $\sqrt{s}$ and q_i are new fit parameters. The number of signal events is consistent with zero at $\sqrt{s} < 1.38$ GeV. The total signal yield in the whole energy range is 2824±290.

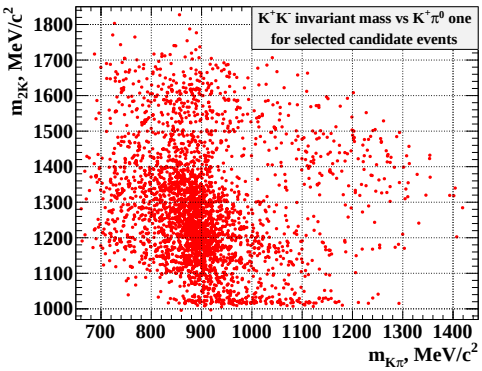

Figure 4. The Dalitz plot distribution for the candidate events selected in the energy range from 1.38 to 2.01 GeV. The presence of K^*K and $\phi\pi^0$ intermediate components is clearly seen.

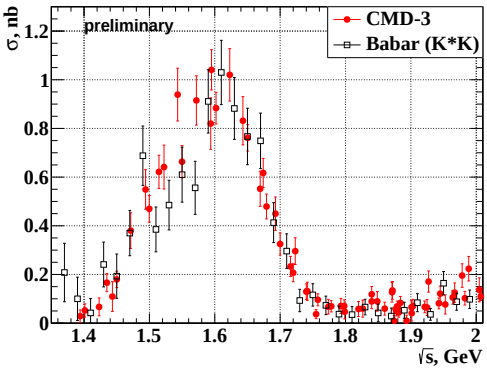

Figure 5. Preliminary cross section of the process $e^+e^- \to K^+K^-\pi^0$ in comparison with the previous BABAR measurement carried out under the assumption that only the K^*K intermediate state contributes to the process.

3 Results

The spectrum in Figure 4 is the Dalitz plot distribution in coordinates of the $K^+\pi^0$ and K^+K^- invariant masses for candidate events that were selected in the whole energy range using a requirement $|M_{\gamma\gamma} - m_{\pi^0}| < 35\,\text{MeV/c}^2$ and the mentioned above criteria with those enhanced for the KF χ^2 and BDT response. As can be seen from Figure 5, the intermediate mechanism $e^+e^- \to K^*K$ dominates and there is a small contribution of the intermediate state $\phi\pi^0$.

The Born cross section at the i-th energy point s_i is determined by the standard formula $\sigma_B(s_i) = N_i/[\epsilon_i L_i(1+\delta_{rc,i})]$, where N_i, ϵ_i, L_i and $\delta_{rc,i}$ denote the number of signal events, detection efficiency, luminosity and radiation correction, respectively. The detection efficiency was determined from MC simulation of the signal process according to the $e^+e^- \to K^*K$ model as this intermediate mechanism is already known to dominate the process. The measured cross section is shown in Figure 5 in comparison with the BABAR result [2]. The latter is obtained assuming that only the K^*K intermediate state contributes to the process under study.

4 Conclusion and acknowledgments

Preliminary results in the study of process $e^+e^- \to K^+K^-\pi^0$ were presented. The event selection algorithm has been developed and the next stage of the analysis includes the determination of efficiency corrections and systematic uncertainties. New data samples are being collected with the VEPP-2000 collider that allows us to increase measurement accuracy.

We would like to thank the Russian Foundation for Basic Research (RFBR), grant 17-52-50064.

References

[1] D. Bisello et al. (DM2), Z. Phys. C - Particles and Fields **52**, 227-230 (1991).
[2] B. Aubert et al. (BABAR), Phys. Rev. D **77** 092002 (2008).
[3] B. I. Khazin et al. (CMD-3), Nucl. Phys. B Proc. Suppl. **376**, 181-182 (2008).
[4] S. Agostinelli et al. (GEANT4), Nucl. Instrum. Methods Phys. Res. A **506**, 250 (2003).